Picosecond Absorption and Resonance Raman Investigation of the Dynamics of the Photoreduction of 4,4′-Bipyridine by Aliphatic Amines in Acetonitrile Solution†

Laurent Boilet,‡ Gotard Burdzinski,§ Guy Buntinx,‡ Christophe Lefumeux,‡ and Olivier Poizat*,‡

LASIR, CNRS, Centre d'Etude et de Recherches Lasers et Applications, bât. C5, Université de Lille I, 59655 Villeneuve d'Ascq Cedex, France, and Department of Physics, University Adam Mickiewicz, Umultowska 85, 61-614 Poznan, Poland

Received: February 8, 2001; In Final Form: April 4, 2001

The photoreduction of 4,4′-bipyridine (44BPY) by 1,4-diazabicyclo[2.2.2]octane (DABCO) and triethylamine (TEA) has been examined in acetonitrile solution by picosecond transient absorption and time-resolved resonance Raman spectroscopy. Both the 44BPY S_1 and T_1 states are quenched by electron transfer via the formation of radical ion pairs. The S_1-state reaction is essentially unproductive as the singlet ion pair undergoes ultrafast intrapair back electron transfer. The T_1-state reaction leads to the anion radical upon reduction by DABCO and to a mixture of anion radical and N-hydro radical upon reduction by TEA. In the latter case, a contact ion pair of 70 ps lifetime is first produced and decays mainly by intrapair proton transfer ($k_{pt} = 1.2 \times 10^{10}$ s^{-1}) and to a minor extent by dissociation into free ions ($k_{dis} = 2.3 \times 10^{9}$ s^{-1}). The free and ion-paired 44BPY anion species have similar absorption spectra but are distinguishable from Raman spectroscopy by slightly different vibrational data. From the analysis of the Raman frequencies, it is suggested that the proton transfer is preceded by a rate-limiting intrapair reorientation step.

Introduction

Intermolecular electron transfer is an elementary reaction involved in many physical, chemical, and biological processes. In solution, electron-transfer results in the formation of radical ion pairs which evolve by dissociation into free ions in competition with intra-pair charge recombination. The separation of the product radical ions is the essential step toward irreversible chemical changes. For this reason, determining the parameters governing the dynamics of evolution of the ion pair is a most important aspect of the research on electron transfer.

The photoreduction of benzophenone by amines has been considerably studied as a prototypical reaction of intermolecular electron transfer in solution.[1] Recent results obtained by femtosecond−picosecond absorption spectroscopy indicate that radical ion pairs with different geometrical structures are produced depending on the spin nature—singlet or triplet—of the precursor excited state, the structure of the amine, and the nature of the solvent. However, the real structure of these associated species and the dynamics of charge separation and charge recombination are still the object of debate.

4,4′-Bipyridine (44BPY) provides an interesting alternative model molecule for investigating the mechanism of photoinduced electron transfer in solution. In a previous work based on nanosecond−microsecond transient absorption and Raman scattering experiments,[2] we found that 44BPY is photoreduced via the lowest triplet state by 1,4-diazabicyclo[2.2.2]octane (DABCO) and triethylamine (TEA) in acetonitrile to yield the anion radical 44BPY$^{-\bullet}$ ($R^{-\bullet}$) and its monoprotonated form, the N-hydro radical 44BPYH$^{\bullet}$ ($RH^{\bullet}$), respectively, which are the analogues of the anion and ketyl radicals produced upon photoreduction of benzophenone. The transient UV−visible absorption and resonance Raman spectra of the 44BPY lowest excited singlet S_1 $n\pi^*$[3,4] and triplet T_1 $\pi\pi^*$[2,5] states and reduced anion radical[2,6] and N-hydro radical[5,7−9] species have been well identified. They provide well-defined and specific spectroscopic signatures for these transient species. Detailed information on the electronic configuration and geometrical structure of these species has been obtained with the help of quantum chemical calculation.[10,12] This ensemble of results represents a valuable basis set of data for starting a comprehensive mechanistic investigation of the photoinduced electron-transfer process in this system. We present here an experimental investigation of the picosecond dynamics of photoreduction of 44BPY by DABCO and TEA in acetonitrile by using transient absorption and time-resolved Raman spectroscopy.

Experimental Section

4,4′-bipyridine (44BPY), triethylamine (TEA), and 1,4-diazabicyclo[2.2.2]octane (DABCO) were purchased from Aldrich. TEA was distilled, and 44BPY was sublimed at 80 °C in vacuo prior to each measurement. Acetonitrile (Prolabo, spectrophotometric grade) and DABCO were used as received. All measurements were performed at $\sim 10^{-3}$ M concentration in 4,4′-bipyridine.

The subpicosecond transient absorption and picosecond Raman scattering experiments have already been described.[3,4,13] Briefly, they were carried out by using a 1 kHz Ti-sapphire laser system based upon a Coherent (MIRA 900D) oscillator and a BM Industries (ALPHA 1000) regenerative amplifier. This system was set in a femtosecond configuration for all absorption measurements. Tripling the initial 90 fs pulses at 800 nm (0.5 mm BBO crystal) provided the pump excitation at 266 nm. Its

† This work was presented at the PP2000 in Costa do Estoril, Portugal, honoring Professor Ralph Becker's contributions.

* Corresponding author. Fax: +33-320434085. E-mail: poizat@univ-lille1.fr.

‡ Université de Lille I.

§ University Adam Mickiewicz.

10.1021/jp010504z CCC: $20.00
Published on Web 05/30/2001

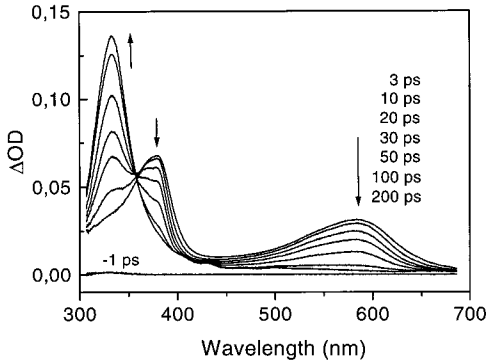

Figure 1. Transient absorption spectra of 44BPY (10^{-3} M) in acetonitrile at different delay times (0−200 ps) after 266 nm excitation.

power was limited to 10−20 μJ per pulse (1.0−2.0 mJ/cm^2). A probe white light continuum pulse was generated at 800 nm in a CaF_2 plate. The probe pulse was delayed in time relative to the pump pulse using an optical delay line (Microcontrol model MT160-250PP driven by an ITL09 controller, precision ±1 μm). The overall time resolution (fwhm of the pump−probe intensity cross-correlation) is estimated to be about 300 fs from the two-photon absorption rise time in pure hexane. The time dispersion of the continuum light over the 300−700 nm region of analysis is about 0.8 ps. The transmitted light was analyzed by a CCD optical multichannel analyzer (Princeton Instrument LN/CCD-1340/400-EB detector + ST-138 controller). Samples were circulating in a flow cell with 2.5 mm optical path length. Data were accumulated over 3 min (~180 000 pump−probe sequences).

For the Raman measurements, the laser source was set in a picosecond configuration. Pump pulses at 253 nm (~15 μJ, 20 mJ/cm^2 per pulse) and probe pulses at 380 nm (~5 μJ) were obtained by frequency tripling and doubling, respectively, the Ti-sapphire fundamental tuned at 760 nm. The pump−probe cross correlation fwhm was ~4 ps. Scattered light was collected at 90° to the incident excitation and sent through a Notch filter into a home-built multichannel spectrometer coupled to a CCD optical multichannel analyzer (Princeton Instrument LN/CCD-1100-PB−UV/AR detector + ST-138 controller). The flowing jet sampling technique was adopted (1 mm diameter jet). The wavenumber shift was calibrated using the Raman spectra of indene. Data collection times were 10−20 min. In all absorption and Raman measurements, the pump−probe polarization configuration was set at the magic angle.

Results

A. Reduction by DABCO. Transient absorption spectra of solutions of 44BPY (10^{-3} M) and DABCO in acetonitrile were recorded for four DABCO concentrations (0.1, 0.3, 0.5, and 0.8 M) at different times in the 0−1500 ps range, following subpicosecond excitation at 266 nm. This excitation falls within a strong $\pi\pi^*$ absorption band of 44BPY (ϵ_{266} = 7500 M^{-1} cm^{-1}). In the absence of DABCO (Figure 1), the time evolution of the spectra is characteristic of the intersystem crossing process (ISC) from the lowest excited S_1 state of 44BPY (380 and 580 nm bands) to the triplet-state T_1 (330 nm band)[3]. By assuming that ISC is the only significant decay process of S_1 ($\phi_{ISC} = 1$[3]), one obtains a rate constant k_{ISC} of (2.3 ± 0.1) × 10^{10} s^{-1}. The T_1 state is stable on this time scale (lifetime 70 μs[2]).

Upon the addition of 0.3 M DABCO (Figure 2), we observe that the 44BPY S_1 spectrum decays faster than the spectrum in pure acetonitrile and that the relative intensity of the appearing T_1-state spectrum is much weaker. The shortening of the S_1 lifetime and the reduction of the T_1 yield indicate clearly that the S_1 state is partly quenched by DABCO. At times longer than 70 ps (Figure 2, part B), the T_1-state spectrum decays, and a new spectrum, a sharp band at 381 nm and a broad signal with maxima around 555, 580, and 638 nm, appears concomitantly. This spectrum is typical of the anion radical,[2] in agreement with our previous observation from nanosecond experiments that the T_1 state is quenched by electron transfer from DABCO. This spectrum is comparable to that obtained by chemical reduction of 44BPY with metallic potassium in tetrahydrofuran.[6] No spectral change in this anion spectrum is perceptible in the 70−1500 ps time domain. It can be seen that although the S_1 state is notably quenched, the intensity of the anion spectrum at the end of the S_1 decay, i.e., in the 50−70 ps domain, seems surprisingly weak in comparison with the contribution of the anion spectrum appearing later from the T_1 state, as if the reaction from S_1 were essentially unproductive. This point is difficult to evaluate more precisely without a quantitative analysis of the observed kinetics since the absorption bands of the anion radical and S_1 state are superimposed in both the UV and visible ranges and differ only by a more pronounced vibronic structure in the case of the ionic species.

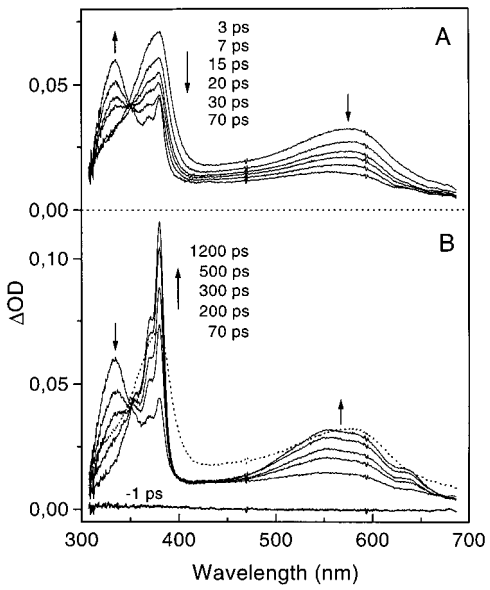

Figure 2. Transient absorption spectra of a solution of 44BPY (10^{-3} M) and DABCO (0.3 M) in acetonitrile at different delay times after 266 nm excitation: (A) the 0−70 ps time range and (B) the 70−1200 ps time range.

Figure 3 shows the time evolution of the Raman spectra recorded at 380 nm, that is, in optimum resonance conditions for both the S_1 state and the anion but in poor resonance with the T_1-state absorption. As expected, these spectra show exclusively the contribution of the resonant S_1 state and anion species. Owing to the high spectral specificity of the vibrational spectroscopy, these two species can be clearly distinguished, for instance, in the 1600 cm^{-1} region, where the two peaks at 1602 and 1566 cm^{-1} (30 ps spectrum) can be ascribed to the characteristic phenyl-type ring deformation mode 8a of the anion radical[2,10] and excited S_1-state[4,12] species, respectively. Two other typical anion vibrations are the ring modes 12 at 983 cm^{-1} and 1 at 738 cm^{-1}.[2,10] The time evolution of the intensity of these two components confirms without ambiguity that the anion radical is essentially formed after complete decay of the S_1 state, that is, from the T_1 state. On the other hand, repeated experiments reveal that the frequency of the anion radical ring deformation modes 8a and 12 show a slight but constant upshift

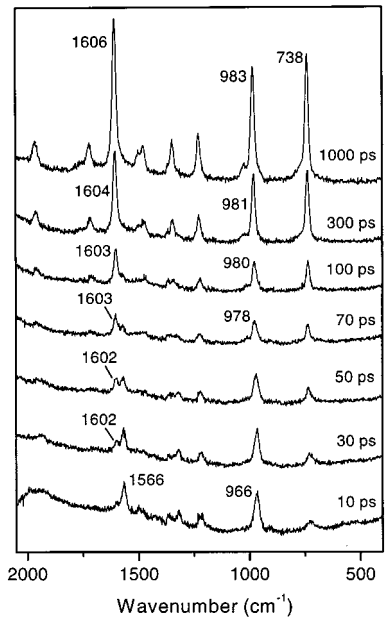

Figure 3. Time-resolved resonance Raman spectra of a solution of 44BPY (10^{-3} M) and DABCO (0.4 M) in acetonitrile probed at 380 nm at different delay times (10−1000 ps) after pump excitation at 253 nm. The probe-only spectrum (solvent and ground-state peaks) has been subtracted to all spectra. Some characteristic Raman frequencies are indicated.

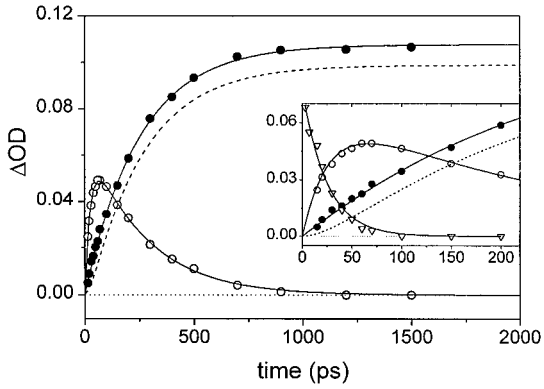

Figure 4. Time dependence of the extracted contributions of the T_1-state absorption at 335 nm (○) and anion radical absorption at 381 nm (●) and the best fit (solid lines) based on reaction Scheme 1 (see the text) for a solution of 44BPY (10^{-3} M) and DABCO (0.3 M) in acetonitrile excited at 266 nm. The inset shows an enlargement of the early time (0−200 ps) kinetics, together with the contribution of the S_1-state absorption at 380 nm (▽). The dashed line is the anion radical kinetics calculated in the assumption of an exclusive T_1-state origin.

of about 4−6 cm^{-1} as the time increases from 30 to 1000 ps. This effect cannot be ascribed to vibrational relaxation since this phenomenon does not exceed 50 ps in solution. Its origin is discussed later.

To get a more quantitative picture of the reaction mechanism, we analyzed the observed absorption spectra in Figure 2 into three contributions according to reference spectra for the S_1, T_1, and anion radical species and fitted the time evolutions related to these contributions with a kinetic model. The reference spectra used in this procedure were the anion spectrum observed after complete quenching of the T_1 state (1200 ps spectrum in Figure 2 for example) and the S_1- and T_1-state spectra recorded at 3 and 200 ps, respectively, in the absence of DABCO (Figure 1). The result is shown in Figure 4, together with the best calculated fit according to the reaction model of Scheme 1.

This model assumes that both the S_1 and T_1 states are

SCHEME 1

$$S_1 \xrightarrow{k_{ISC}} T_1$$

$$S_1 + \text{DABCO} \xrightarrow{k_r^1} \begin{cases} R^{-\cdot} & (\Phi_{et}^1) \\ S_0 & (\Phi_{deac}^1) \end{cases}$$

$$T_1 + \text{DABCO} \xrightarrow{k_r^3} R^{-\cdot}$$

quenched by DABCO with rate constants k_r^1 and k_r^3, respectively, and that the quantum yield ϕ_{et}^3 of formation of the anion radical ($R^{-\bullet}$) from the T_1 state is equal to unity. On the other hand, it includes a quenching-induced deactivation pathway of the S_1 state (quantum yield $\phi_{deac}^1 = 1 - \phi_{et}^1$). The k_{ISC} value in Scheme 1 was considered to be the same as that determined in the absence of DABCO (2.3×10^{10} s^{-1}). The exact values of the extinction coefficients are not known but an approximate intensity ratio of 1:2:3.2 was considered for the S_1, T_1, and anion absorption maxima at 380, 335, and 381 nm, respectively. The relative S_1 and T_1 coefficients were estimated from the ratio of the T_1 band intensity at the end of the $S_1 \rightarrow T_1$ kinetics in the absence of DABCO and of the initial S_1 band intensity obtained by extrapolating the exponential decay fit of the S_1 absorption to time zero. The relative T_1 and anion coefficients were deduced similarly from the initial T_1 absorption and final anion absorption in the presence of DABCO. The calculated kinetics were normalized to the experimental data according to the initial S_1-state absorption.

If the quenching reaction of S_1 by DABCO is supposed to yield the anion radical with a 100% efficiency ($\phi_{et}^1 = 1$), the rising kinetics calculated for the anion at short time cannot be adjusted to the experimental kinetics: it is much too fast and appears close to that observed for the T_1 state. Moreover the final amount of anion is predicted almost twice as large as that observed experimentally. On the contrary, if the anion is assumed to originate exclusively from the T_1 state, ($\phi_{deac}^1 = 1$) the calculated anion kinetics (dashed line in Figure 4) starts unavoidably too slowly in the 0−30 ps range (see the inset in Figure 4) and underestimates the final amount of anion. The best fit is obtained for a quantum yield of $\phi_{et}^1 = 0.08 \pm 0.03$, indicating that 90−95% of the S_1 molecules that are quenched by DABCO are deactivated to the ground state. This confirms our above expectation that the quenching process of S_1 is essentially unproductive.

The decay kinetics of T_1 and the corresponding growing kinetics of the anion above 70 ps are monoexponential, and the reaction rate constant k_r^3 varies linearly with the DABCO concentration, as expected for a pseudo-first-order kinetics ($k_r^3 = k_q^3 \times$ [DABCO]). A Stern−Volmer analysis leads to a quenching rate constant of $k_q^3 = (1.2 \pm 0.2) \times 10^{10}$ M^{-1} s^{-1}, which is in reasonable agreement with the value of 0.9×10^{10} M^{-1} s^{-1} found previously from nanosecond experiments for low concentrations of DABCO (10^{-5}−10^{-4} M range). The quenching process is thus still following a diffusional regime for DABCO concentration as high as 0.1−0.8 M. A roughly linear plot as a function of the DABCO concentration is also obtained for the reaction rate at the S_1 state: $k_r^1 = k_q^1 \times$ [DABCO], with $k_q^1 = (3.5 \pm 1.5) \times 10^{10}$ M^{-1} s^{-1}. Despite an important imprecision on the k_q^1 value due to the difficulty of measuring properly the intensity of the overlapping S_1 and anion absorption features, this value seems higher than the diffusional rate constant in acetonitrile ($k_{diff} = 2 \times 10^{10}$ M^{-1} s^{-1}). Therefore,

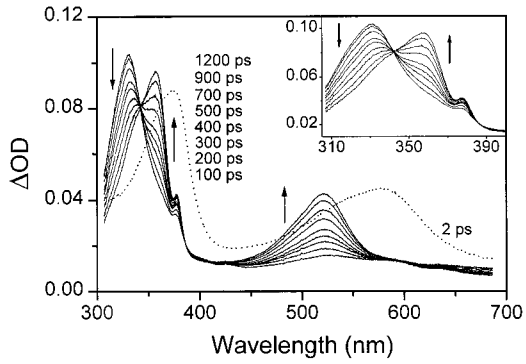

Figure 5. Transient absorption spectra of a solution of 44BPY (10^{-3} M) and TEA (0.4 M) in acetonitrile at different delay times in the 100−1200 ps range after 266 nm excitation. The 2 ps spectrum is also shown (dotted line) for comparison. The inset shows an enlargement of the 310−400 nm region.

the S_1-state quenching reaction is probably not a purely diffusion-limited process at such high DABCO concentration. It is probable that some of the donor molecules are close enough to a ground-state 44BPY molecule for undergoing static electron-transfer quenching after excitation. As a matter of fact, all the situations between pure static and pure diffusional quenching can be expected. However, the fact that no instantaneous rising component is perceptible at short time in the appearance kinetics of the anion radical indicates that there is no direct intra-complex charge transfer upon excitation.

Finally, on the basis of the reaction Scheme 1, it has been possible to reproduce directly, by using the set of parameters determined above ($k_q^1 = (3.5 \pm 1.5) \times 10^{10}$ M^{-1} s^{-1}, $k_q^3 = (1.2 \pm 0.2) \times 10^{10}$ M^{-1} s^{-1}, and $k_{ISC} = (2.3 \pm 0.1) \times 10^{10}$ s^{-1}, $\phi^1_{et} \approx 0.08$, $\phi^3_{et} = 1$), the profile and the relative amplitude of the kinetics of the S_1 and T_1 states and the anion radical absorption for the four DABCO concentrations experienced.

B. Reduction by TEA. Five solutions of 44BPY (10^{-3} M) and TEA (0.2, 0.4, 0.6, 0.75, and 0.9 M) in acetonitrile were investigated by transient absorption spectroscopy. The time-evolution of the spectra in the 0−100 ps time domain reveal, as in the case of DABCO, a linear decrease of the S_1-state lifetime and of the T_1-state yield as the TEA concentration is increased. A Stern−Volmer analysis leads to a quenching rate constant of $k_q^1 = (1.9 \pm 0.6) \times 10^{10}$ M^{-1} s^{-1}, nearly equal to the diffusional rate constant. The T_1-state lifetime is also linearly shortened upon the addition of TEA, with a quenching rate constant of $k_q^3 = (4.2 \pm 0.3) \times 10^9$ M^{-1} s^{-1}. This value is close to that found in the nanosecond range for much lower TEA concentrations (4×10^9 M^{-1} s^{-12}). Figure 5 shows a series of transient absorption spectra recorded for various pump−probe delays in the 100−1200 ps range for [TEA] = 0.4 M. The spectrum appearing concomitantly to the decay of the T_1 spectrum is clearly different to that observed with DABCO (Figure 2B). The main bands at 360 and 524 nm are characteristic of the N-hydro radical RH• of 44BPY,[5,8,9] which is the N-protonated form of the anion radical. A weak shoulder at 381 nm indicates that the anion radical is probably also produced to a much lower extent. An apparent isosbestic point is observed at 342 nm, between the T_1-state and N-hydro absorption bands, suggesting at first sight that the main reaction at the T_1 state is hydrogen atom abstraction from TEA. This hypothesis is nevertheless questionable in view of the high value of the T_1-state quenching rate constant k_q^3 found above. In fact, H atom abstraction by 44BPY in the T_1 state was found to occur from alcohols and alkanes at rate constants of $(1-5) \times 10^5$ M^{-1} s^{-1}.[5]

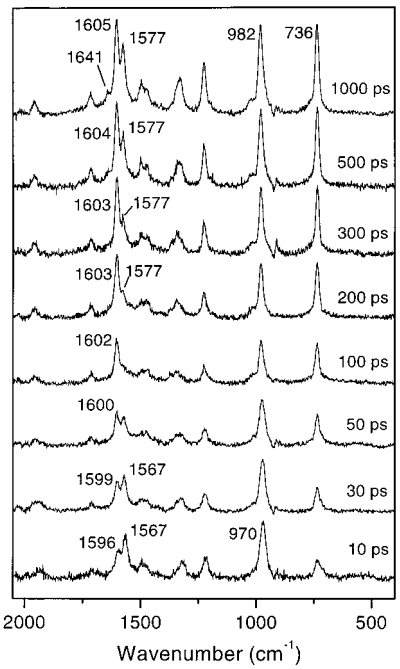

Figure 6. Time-resolved resonance Raman spectra of a solution of 44BPY (10^{-3} M) and TEA (0.4 M) in acetonitrile probed at 380 nm at different delay times (10−1000 ps) after pump excitation at 253 nm. The probe-only spectrum (solvent and ground-state peaks) has been subtracted to all spectra. Some characteristic Raman frequencies are indicated.

Figure 6 shows some resonance Raman spectra recorded at different pump−probe delays in the 10−1000 ps range with the same solution as that for the absorption measurements in Figure 5 (0.4 M TEA). The 10 ps spectrum is mainly characteristic of the S_1 state of 44BPY (typical bands at 1567 and 970 cm^{-1}). As the delay time is increased, the decay of the S_1 state is manifested by the disappearance of the 1567 cm^{-1} line, and the growing of the anion radical spectrum (lines around 1600, 982, and 736 cm^{-1}) is clearly visible. A second rising contribution to the spectra in Figure 6 is represented by the lines at 1641 and 1577 cm^{-1} (1000 ps spectrum), which are characteristic of the N-hydro radical RH•.[7] The fact that the Raman spectrum of the anion appears more intense than the radical spectrum whereas the anion absorption (Figure 5) is much weaker than the radical one can be imputed to a higher-resonance Raman enhancement of the anion spectrum. In fact, the Raman probe excitation at 380 nm is in optimum resonance with the 381 nm anion absorption but almost out of resonance with the 360 nm radical absorption. Thus, these results confirm definitely the identity of the three transient species involved in the photoreduction reaction by TEA. From a kinetics point of view, the Raman spectrum of the anion shows a significant increase over the first 300 ps period, followed by a much slower increase in the 300−1000 ps interval. On the other hand, the radical spectrum is seen only after 150 ps and increases continuously from 150 to 1500 ps. The appearance kinetics of the radical thus seems somewhat retarded relative to the anion kinetics. As with DABCO, the frequency of the anion mode 8a increases slightly from 10 to 1000 ps, whereas the corresponding N-hydro radical mode frequency remains constant.

To get a more quantitative knowledge of the kinetics, we analyzed the experimental absorption spectra in the same way as above for the reduction by DABCO. The specific contributions of the T_1 state, anion radical, and N-hydro radical to the

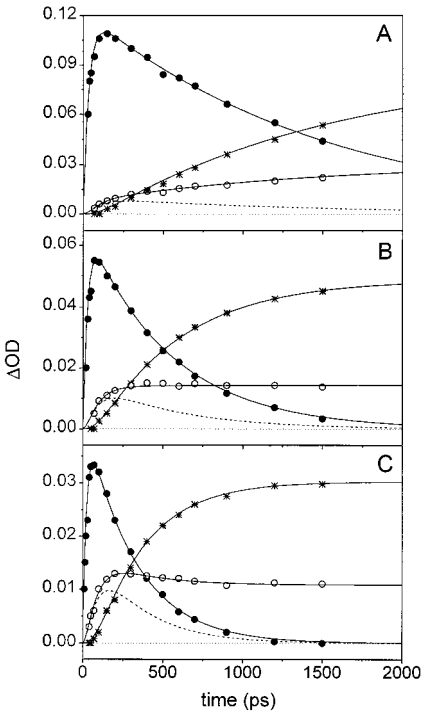

Figure 7. Time dependence of the extracted contributions of the T_1-state absorption at 335 nm (●), anion radical absorption at 335 nm (○), and N-hydro radical absorption at 381 nm (∗) and the best fit (solid lines) based on reaction Scheme 3 (see the text) for acetonitrile solutions of 10^{-3} M 44BPY and (A) 0.2 M DABCO, (B) 0.6 M DABCO, and (C) 0.9 M DABCO excited at 266 nm. The dashed line is the calculated kinetics of the ion pair contribution of the anion radical.

absorption kinetics at 335, 381, and 360 nm, respectively, are plotted in Figure 7 for three TEA concentrations. The anion evolution is particularly sensitive to the TEA amount. At 0.2 M TEA (Figure 7A), the appearance kinetics of the anion shows two stages: a rapid, low-amplitude growth below 200 ps, followed by a slight increase over the 200−1500 ps domain. At 0.9 M TEA (Figure 7C), the short-time rising component has a stronger amplitude and is followed by a slight decrease from 200 to 900 ps and then by a stable residual signal after 900 ps. In all cases, the radical appearance onset is delayed relative to the anion kinetics, in agreement with the kinetic evolution observed by Raman.

To fit these experimental kinetics, we used the k_{ISC} constant and relative S_1, T_1, and anion absorption strengths adopted for Scheme 1 and the k_q^1 and k_q^3 quenching rate constants found above. A relative extinction coefficient of 1.75 was assessed for the RH• radical absorption at 360 nm, on the basis of the 3.2 value of the anion absorption at 381 nm, from the following measurement: in binary water−acetonitrile solutions, the anion radical produced initially upon the photoreduction of 44BPY by DABCO is then protonated by water.[14] Comparing the initial anion and final radical absorption intensities gives an estimate of their relative absorption strengths. To be able to fit the short-time kinetics (0−70 ps) for which the contribution of the S_1-state reactivity is dominant, it was necessary to introduce, as in Scheme 1 for the reduction by DABCO, a quenching-induced deactivation route of the S_1 state with a high efficiency (quantum yield 0.9−0.95). At times longer than 70 ps, where the kinetics are mainly characteristic of the T_1 reactivity, it was impossible to get a satisfying fit of the anion and radical kinetics by assuming a reaction model where these species arise independently from the T_1 state by two competitive quenching process (Scheme 2).

SCHEME 2

$$T_1 + TEA \xrightarrow{e^- \text{ transfer}} R^{-\cdot}$$

$$T_1 + TEA \xrightarrow{H^\cdot \text{ transfer}} RH^\cdot$$

SCHEME 3

$$S_1 \xrightarrow{k_{ISC}} T_1$$

$$S_1 + TEA \xrightarrow{k_r^1} \begin{cases} R^{-\cdot} & (\Phi_{et}^1) \\ S_0 & (\Phi_{deac}^1) \end{cases}$$

$$T_1 + TEA \xrightarrow{k_r^3} (R^{-\cdot},\ TEA^{+\cdot})$$

$$(R^{-\cdot},\ TEA^{+\cdot}) \xrightarrow{k_{dis}} R^{-\cdot}_{solv} + TEA^{+\cdot}_{solv}$$

$$(R^{-\cdot},\ TEA^{+\cdot}) \xrightarrow{k_{pt}} RH^\cdot + TEA^\cdot$$

The only way to reproduce correctly the kinetics observed for the anion and radical species was to consider the sequential electron-transfer-proton-transfer reaction model described in Scheme 3.

In this model, the 44BPY triplet states is quenched by electron transfer to yield a radical ion pair (rate $k_r^3 = k_q^3 \times$ [TEA]). This reaction is followed by intrapair proton transfer (rate k_{pt}) from the amine cation ($TEA^{+\bullet}$) to the 44BPY anion ($R^{-\bullet}$), leading to the neutral N-hydro radical ($RH^\bullet$) and amine radical TEA(−$H^\bullet$), in competition with ion-pair dissociation into the free, solvated ions (rate k_{dis}). The observed anion kinetics is assumed to be the sum of the ion pair and free anion contributions. The best fit is shown in Figure 7 for three TEA concentrations. It is obtained for an ion-pair lifetime of 70 ps and an intrapair proton transfer versus charge separation efficiency of 84%/16%. This corresponds to ion pair decay rate constants of $k_{pt} = (1.2 \pm 0.3) \times 10^{10}$ s^{-1} and $k_{dis} = (2.3 \pm 0.3) \times 10^9$ s^{-1}. This set of parameters allows reproducing correctly the shape and relative amplitude of the kinetics of the S_1, T_1, $R^{-\bullet}$, and $RH^\bullet$ transient species for the five TEA concentrations experienced. The calculated ion pair kinetics is shown in Figure 7 by a dashed line. At high TEA concentration (Figure 7C), the ion pair is efficiently produced at short time and can accumulate significantly. This accounts for the slight maximum observed around 200 ps in the anion kinetics.

Such sequential electron−proton transfer has been found in the photoreduction of ketones by tertiary amines.[1,15] In fact, the cation radical of tertiary amines is much more acidic than the neutral molecule[16] and undergoes α-CH deprotonation to produce the corresponding α-amino radical.[15,17] This intrapair reaction in Scheme 3 is favored by the high basicity of the 44BPY anion radical (pK_a ($RH^\bullet/R^{-\bullet}$) > 14[18]). The absence of the deprotonation step in the case of DABCO denotes a low cation radical acidity due to the rigidity of the bridged skeleton, which cannot rearrange to stabilize the α-amino radical form.[19]

Discussion

The fast and chemically unproductive deactivation of the nπ^* S_1 state in the presence of amines can have two origins. First, it can be due to the presence of a conical intersection between the S_1 and S_0 energy surfaces located along the excited-state

TABLE 1: Summary of the Kinetic Parameters for the Reactions Involved in the Photoreduction of 44BPY by the Amines DABCO and TEA

reaction		DABCO	TEA
$S_1 \rightarrow T_1$	k_{ISC}	2.3×10^{10} s^{-1}	2.3×10^{10} s^{-1}
$S_1 + \text{amine} \rightarrow {}^1[R^{-\bullet}, \text{amine}^{+\bullet}]$	k_q^1	3.5×10^{10} M^{-1} s^{-1}	1.9×10^{10} M^{-1} s^{-1}
${}^1[R^{-\bullet}, \text{amine}^{+\bullet}] \rightarrow S_0 + \text{amine}$	k_{ret}^1	$>10^{11}$ s^{-1}	$> 10^{11}$ s^{-1}
	Φ_{ret}^1	~0.92	~ 0.9
${}^1[R^{-\bullet}, \text{amine}^{+\bullet}] \rightarrow (R^{-\bullet})_{solv} + (\text{amine}^{+\bullet})_{solv}$	k_{dis}^1	$>10^{10}$ s^{-1}	$>10^{10}$ s^{-1}
	Φ_{dis}^1	~0.08	~0.1
$T_1 + \text{amine} \rightarrow {}^3[R^{-\bullet}, \text{amine}^{+\bullet}]$	k_q^3	1.2×10^{10} M^{-1} s^{-1}	4.2×10^9 M^{-1} s^{-1}
${}^3[R^{-\bullet}, \text{amine}^{+\bullet}] \rightarrow RH^{\bullet} + \text{amine}(-H^+)$	k_{pt}^3		1.2×10^{10} s^{-1}
	Φ_{pt}^3	~0	0.84
${}^3[R^{-\bullet}, \text{amine}^{+\bullet}] \rightarrow (R^{-\bullet})_{solv} + (\text{amine}^{+\bullet})_{solv}$	k_{dis}^3	(~2.3×10^9 s^{-1})[a]	2.3×10^9 s^{-1}
	Φ_{dis}^3	~1	0.16

[a] Value estimated by analogy with that measured in the case of TEA.

electron transfer reaction pathway, as recently demonstrated for the quenching of the nπ^* excited states of azoalkanes by amines.[20] From quantum calculation of the minimum energy reaction path, the authors show that the mechanism involves the formation of an exciplex with limited charge-transfer character close to the conical intersection. In this case, the reaction is thus aborted after partial charge transfer through radiationless deactivation. Such a charge transfer-induced quenching process is expected for systems with low driving force of electron transfer and should be characterized by quenching rate constants far below the diffusion-controlled limit,[20] which is not the case in the quenching of S_1 44BPY by DABCO and TEA. The high values of k_q^1 found above ($k_q^1 \geq k_{diff}$) are rather indicative of the formation of an ion pair with full electron-transfer character. An estimate of the driving force can be inferred from the reduction potential of 44BPY (E_{red} vs SCE = -1.83 V[21]). The energy of the S_1 state of 44BPY is not known precisely but can be approximated from low-temperature absorption measurements reported by McAlpine for 44BPY diluted in a crystal of biphenyl. The author ascribed the lowest energy band (30300 cm^{-1}) to a $S_0 \rightarrow S_1$ (nπ^*) vibronic component but expressed a doubt about its assignment to the 0$-$0 transition.[22] A singlet energy of $E(S_1) \leq 86$ kcal mol^{-1} (3.7 eV) is thus deduced. Accordingly, a lower limit for the free energy of electron-transfer quenching of the S_1 state is found from the Rehm$-$Weller theory[23] to be $\Delta G_{ET}(S_1) = -1.0$ eV in the case of DABCO ($E_{ox} = 0.87$ V vs SCE) and -0.9 eV in the case of TEA ($E_{ox} = 0.96$ V vs SCE). These values are clearly more exergonic than those in the free energy range ($\Delta G_{ET} > \sim -0.4$ eV) generally considered as characteristic of the formation of an exciplexe or a contact ion pair (CIP).[24$-$27] For $\Delta G_{ET} < \sim -0.4$ eV, the transfer of electron occurs before the acceptor and donor species are in close contact and leads to the formation of a solvent-separated ion pair (SSIP), bypassing the CIP. This confirms that the deactivation of the 44BPY S_1 state by amines is not be due to a charge transfer-induced quenching process. It is thus more likely ascribable to an ultrafast charge recombination following the formation of the ion pair. In fact, this process is spin-allowed, whereas it requires spin conversion in the case of the triplet radical ion pair and thus does not occur on the picosecond time scale. The S_1 state being deactivated at 90$-$95%, the intrapair back electron transfer can be estimated to be 10$-$20 times faster than the dissociation of the singlet radical ion pair. This ion pair being not characterized in the present data, its lifetime remains unknown, but it is certainly shorter than 10 ps. In conclusion, Table 1 gives a summary of the whole set of reactions involved in the photoreduction of 44BPY by DABCO and TEA and the corresponding kinetic parameters.

TABLE 2: Observed Raman Frequencies (in cm^{-1}) for Two Typical Vibrations of the 44BPY Anion Radical

		acetonitrile		
normal mode[a]	amine donor	ion pair[b]	free ion[c]	water[d]
8a	DABCO	1602	1606	1611
8a	TEA	1600	1605	1611
12	DABCO	978	983	992
12	TEA	978	982	992

[a] Mode assignment from ref 10. [b] Pump$-$probe delay time, 50 ps. [c] Pump$-$probe delay time, 1000 ps. [d] From ref 14.

The absorption spectra of the anion engaged in the pair and of the free anion are not distinguishable. In the case of reduction by DABCO, there is no information in the observed kinetics, allowing the characterization of the presence of an ion pair. However, in the case of reduction by TEA, the triplet ion pair kinetics could be determined from the global anion radical kinetics because of the presence of a specific intrapair reaction. Obviously, a similar triplet radical ion pair is expected to be formed with DABCO as with TEA. By assuming comparable values of the ion pair dissociation rate constant with both amines ($k_{dis} \approx 2.3 \times 10^9$ s^{-1}), we predicted a triplet ion pair lifetime of 400 ps in the case of DABCO. Consider now the data obtained from Raman experiments. With TEA as well as with DABCO, a slight frequency increase has been remarked for some Raman ring deformation modes of the 44BPY anion radical over the 50$-$1000 ps time range. This frequency increase denotes a slight modification of the π-electron density distribution in the pyridyl rings due to some kind of relaxation process. It is reasonable to correlate this effect to the escape of the anion from the ion pair which arises in the same time domain. It can be related to the disappearance of the electronic interaction between the amine cation and 44BPY anion as the ion pair dissociates and to the concomitant ion solvation effect. This observation shows that vibrational spectroscopy is sensitive enough to weak intermolecular interactions to be able to distinguish a free ion from its analogue engaged in an ion pair. In summary, the characteristic Raman frequencies observed for the two types of anion species are reported in Table 2. The corresponding values found elsewhere[14] for the anion in water are also given for comparison.

The high value of the rate constant for intrapair proton transfer between the 44BPY anion and TEA cation ($k_{pt} = 1.2 \times 10^{10}$

s^{-1}) suggests that the two ionic partners are in contact with each others, which implies that the triplet ion pair formed upon photoreduction in acetonitrile is a CIP. This conclusion is in agreement with the driving force estimated for the process according to the Rehm−Weller theory.[23] Although the energy of the 44BPY T_1 state is not known, an approximate value of $E(T_1) \approx 70$ kcal mol^{-1} (3.04 eV) can be assumed from the identification of the ν_{00} ($T_1 \rightarrow S_0$) transition at 24630 cm^{-1} in the low-temperature phosphorescence spectrum.[28] This value is in accord with the vertical and adiabatic $S_0 \rightarrow T_1$ energy values of 72 and 66 kcal mol^{-1}, respectively, predicted from ab initio calculation.[29] On this basis, the free energy of electron-transfer quenching of the T_1 state by DABCO and TEA is predicted as $\Delta G_{ET}(T_1) \approx -0.34$ and -0.25 eV, respectively. The low exergonicity of the triplet reaction ($\Delta G_{ET}(T_1) > -0.4$ eV) seems plausible in regard to the fact that no electron-transfer reaction is observed with 4-phenylpyridine,[30] which is expected to have a triplet energy comparable to that of 44BPY but is less oxidant by 0.33 V.[31] It confirms the assumption that the triplet-state electron-transfer process involves the formation of a CIP.

Finally, consider the mechanism of the intrapair proton transfer process arising in the triplet CIP in the case of TEA. It is conceivable that the equilibrium geometry of the species for electron transfer is not the same as that for proton transfer. Therefore, a reorientation step is necessarily preceding the intrapair proton-transfer reaction itself. This assumption is in agreement with the two-step mechanism proposed by Dreyer and Peters for the intrapair proton transfer between benzophenone and *N*,*N*-dimethylaniline.[32] We expect that at a configuration favorable to proton transfer, the strongly basic 44BPY anion and the proton donor TEA cation must be H-bonded in the pair. If this reorientation step is fast regarding the actual proton transfer itself, that is, if the proton transfer is the rate-limiting step, the H-bonded configuration should be observed dominantly. On the other hand, if the reorientation step is rate-limiting, that is, if the proton transfer occurs as soon as the species are favorably oriented, the H-bonded configuration must be too short-lived to be observed. As seen in Table 2, the typical Raman frequencies found in acetonitrile for the 44BPY anion radical associated in an ion pair with the TEA cation radical are similar to those observed for the ion pair with the DABCO cation but are significantly lower than those found in protic solvents such as water or alcohols where the anion is hydrogen-bonded to solvent molecules.[14] Moreover, the values found for the free anion radical in acetonitrile are also lower than those in water, in such a way that a frequency decrease can be expected to characterize a process of H-bond breaking. A frequency increase, however, is observed in going from the ion pair to the free ions. The main population of the radical ion pair present in pure acetonitrile can thus be considered as not characterized by an intrapair H-bonded anion−cation configuration. We conclude that the rate-limiting step in the transfer of proton within the 44BPY/TEA contact radical ion pair is mainly the reorganization of the reaction complex. A similar conclusion has been drawn for the intrapair proton transfer between benzophenone and *N*,*N*-dimethylaniline from the analysis of the proton/deuteron isotopic effect on the reaction rate.[32] This means that the evolution of the ion pair is governed by a competition between the dynamics of this reorientation process and the dynamics of dissociation into free ions. About one-fifth of the ion pair population undergoes charge separation before the reorganization dynamics allows the intrapair proton transfer.

Acknowledgment. The authors thank the Groupement de Recherche GDR 1017 from CNRS and the Centre d'études et de Recherches Lasers et Applications (CERLA) for their help in the development of this work. CERLA is supported by the Ministère chargé de la Recherche, Région Nord/Pas de Calais, and the Fonds Européen de Développement Economique des Régions.

References and Notes

(1) See, for example: (a) Devadoss, C.; Fessenden, R. W. *J. Phys. Chem.* **1990**, *94*, 4540. (b) Miyasaka, H.; Morita, K.; Kamada, K.; Nagata, T.; Kiri, M.; Mataga, N. *Bull. Chem. Soc. Jpn.* **1991**, *64*, 3229. (c) Haselbach, E.; Jacques, P.; Pilloud, D.; Suppan, P.; Vauthey, E. *J. Phys. Chem.* **1991**, *95*, 7115. (d) Peters, K. S.; Lee, J. *J. Phys. Chem.* **1993**, *97*, 3761.

(2) Buntinx, G.; Valat, P.; Wintgens, V.; Poizat, O. *J. Phys. Chem.* **1991**, *95*, 9347.

(3) Buntinx, G.; Naskrecki, R.; Poizat, O. *J. Phys. Chem.* **1996**, *100*, 19380.

(4) Didierjean, C.; Dewaele, V.; Buntinx, G.; Poizat, O. *Chem. Phys.* **1998**, *237*, 169.

(5) Poizat, O.; Buntinx, G.; Valat, P.; Wintgens, V.; Bridoux, M. *J. Phys. Chem.* **1993**, *97*, 5905.

(6) Kihara, H.; Gondo, Y. *J. Raman Spectrosc.* **1986**, *17*, 263.

(7) Poizat, O.; Buntinx, G.; Ventura, M.; Lautié, M. F. *J. Phys. Chem.* **1991**, *95*, 1245.

(8) Simic, M.; Ebert, M. *Int. J. Radiat. Phys. Chem.* **1971**, *3*, 259.

(9) Elisei, F.; Mazzucato, U.; Görner, H.; Schulte-Frohlinde, D. *J. Photochem. Photobiol. A* **1989**, *50*, 209.

(10) Ould-Moussa, L.; Poizat, O.; Castella-Ventura, M.; Buntinx, G.; Kassab, E. *J. Phys. Chem.* **1996**, *100*, 2072.

(11) Castella-Ventura, M.; Kassab, E. *J. Raman Spectrosc.* **1998**, *29*, 511.

(12) Dewaele, V.; Buntinx, G.; Poizat, O.; Flament, J.-P.; Kassab, E. *J. Chem. Phys.* **1999**, *110*, 6353.

(13) Didierjean, C.; Buntinx, G.; Poizat, O. *J. Phys. Chem. A* **1998**, *102*, 7938.

(14) Poizat, O.; Buntinx, G.; Boilet, L.; Lefumeux, C. Unpublished results, 2001.

(15) Wagner, P. J. *Top. Curr. Chem.* **1976**, *66*, 1.

(16) Das, S.; von Sonntag, C. *Z. Naturforsch.* **1986**, *416*, 505.

(17) Chow, Y. L.; Danen, W. C.; Nelsen, S. F.; Rosenblatt, D. *Chem. Rev.* **1978**, *78*, 243.

(18) Fessenden, R. W.; Neta, P. *Chem. Phys. Lett.* **1973**, *18*, 14.

(19) Griller, S.; Howard, J. A.; Marriott, P. R.; Scaiano, J. C. *J. Am. Chem. Soc.* **1981**, *103*, 619.

(20) Sinicropi, A.; Pischel, U.; Basosi, R.; Nau, W. M.; Olivucci, M. *Angew. Chem., Int. Ed. Engl.* **2000**, *39*, 4582.

(21) Persaud, L.; Barbiero, G. *Can. J. Chem.* **1991**, *69*, 315.

(22) McAlpine, R. D. *J. Mol. Spectrosc.* **1971**, *38*, 441.

(23) Rehm, D.; Weller, A. *Isr. J. Chem.* **1970**, *8*, 259.

(24) Gould, I. R.; Young, R. H.; Mueller, L. J.; Farid, S. *J. Am. Chem. Soc.* **1994**, *116*, 8176.

(25) Gould, I. R.; Farid, S. *Acc. Chem. Res.* **1996**, *29*, 522.

(26) Vauthey, E.; Högemann, C.; Allonas, X. *J. Phys. Chem. A* **1998**, *102*, 7362.

(27) Vauthey, E. *J. Phys. Chem. A* **2001**, *105*, 340.

(28) Yagi, M.; Matsunaga, M.; Higuchi, J. *Chem. Phys. Lett.* **1982**, *86*, 219.

(29) Castella-Ventura, M.; Kassab, E. Unpublished work, 1999.

(30) Buntinx, G.; Naskrecki, R.; Didierjean, C.; Poizat, O. *J. Phys. Chem. A* **1997**, *101*, 8768.

(31) Tabner, B. J.; Yandle, J. R. *J. Chem. Soc. A* **1968**, 381.

(32) Dreyer, J.; Peters, K. S. *J. Phys. Chem.* **1996**, *100*, 19412.